

Human Apprenticeship Learning via Kernel-based Inverse Reinforcement Learning

Mark A. Rucker^a, Layne T. Watson^b, Laura E. Barnes^a and Matthew S. Gerber^a

^aUniversity of Virginia; ^b Virginia Polytechnic Institute and State University

ARTICLE HISTORY

Compiled December 21, 2024

ABSTRACT

This paper considers if a reward function learned via inverse reinforcement from a human expert can be used as a feedback intervention to alter future human performance as desired (i.e., human to human apprenticeship learning). To learn reward functions two new algorithms are developed: a kernel-based inverse reinforcement learning algorithm and a Monte Carlo reinforcement learning algorithm. The algorithms are benchmarked against well-known alternatives within their respective corpus and are shown to outperform in terms of efficiency and optimality. To test the feedback intervention two randomized experiments are performed with 3,256 human participants. The experimental results demonstrate with significance that the rewards learned from “expert” individuals are effective as feedback interventions. In addition to the algorithmic contributions and successful experiments, the paper also describes three reward function modifications to improve reward function feedback interventions for humans.

1. Introduction

Spare the rod, spoil the child. The impact of environmental feedback on human behavior has long been understood at an intuitive level. However, it wasn’t until the pioneering work of Thorndike and Pavlov in the late nineteenth century, that such intuition began to be formulated as a scientific system of knowledge. Fast forward more than a century and much of the current state of the art in machine learning and robotics draws inspiration from Thorndike’s and Pavlov’s theories in an area of research known as *reinforcement learning* (RL).

In the classic research of Thorndike and Pavlov environmental feedback signals are known. What is not known is how these signals influence animal behavior. Similarly, RL research also assumes an environmental feedback signal is known (i.e., a reward function). What is not known is the optimal behavior for pursuing the reward signal (i.e., an optimal policy). For this reason traditional RL research has focused on methods to learn optimal behavior given a reward signal and experience.

Recently, some researchers have begun to turn the RL field on its head with a new problem formulation, *inverse reinforcement learning* (IRL). The IRL problem assumes that an optimal policy is known and the reward function driving it is unknown. Given these assumptions, IRL techniques seek to learn reward functions from optimal policies.

IRL methods open the door to a new possibility: learning the rewards that drive human behavior. Unfortunately, previous research has shown that human behavior

is the result of both reward-seeking and non-reward-seeking processes (cf. [4]). Such results suggest that truly learning what an individual finds rewarding may not be possible through observation of behavior alone. For this reason, the authors tend to think of IRL human-reward functions simply as information about behavior.

Regardless of what IRL reward functions learned from human behavior may truly represent, it can still be asked how they might be used. This paper demonstrates a new use case: human to human apprenticeship learning via *feedback interventions* (FI's), where an FI is defined as *any external action taken to provide an individual with information about their performance* (cf. [18]).

To evaluate IRL for the FI use case three contributions are made: (1) a new IRL algorithm is developed that is more amenable to human behavior (2) a new RL algorithm is developed to work without any reward shaping and (3) two controlled experiments are conducted test if reward functions representing human behavior can be used as an FI on other human participants.

In what follows, Section 2 provides a very cursory review of related research. Section 3 covers preliminary technical terms and formulations. Section 4 describes the algorithms developed for the experiment. Section 5 outlines the experimental design and setup. Section 6 details the results of the experiment. And Section 7 gives a brief summary of the contributions of this paper along with future research directions.

2. Related Work

Several methods have been previously proposed to solve the IRL problem. In a gross generalization these methods can be classified as either score-based optimization methods [32, 1, 37, 17, 23] or probabilistic/likelihood methods [36, 55, 25, 53, 35, 10].

Approaches in the former camp tend to scale well with complex IRL problems but have more constraints placed on the shape of their reward functions and policies. Approaches in the latter camp tend to have greater freedom in their reward functions and policies but often don't scale well as IRL problems increase in complexity. Given the nuance of human behavior, and the size of the state space in our MDP, a new method was needed which was both efficient and flexible.

For the IRL algorithm developed in this paper an approach from the first group, [1], is selected for its efficiency and extended via kernel methods [41] to relax reward function constraints. This IRL approach is benchmarked against a score based algorithm [1] and a likelihood based method [25], demonstrating exponential gains in efficiency can be made with small concessions in accuracy.

The developed IRL algorithm also requires solving the RL problem (i.e., finding an optimal policy given a reward). Therefore a new RL algorithm is designed, utilizing recent advances in RL with function approximation [28, 34, 20, 54], and used in our IRL algorithm, where little is known about the reward a priori. The RL algorithm is benchmarked against two least-squares temporal difference (LSTD) [8] policy iteration algorithms [20, 54] and is shown to have a greater expected performance given 2,000 randomly generated reward functions.

Experiments in [11] suggest that LSTD is still state of the art for policy evaluation in on-policy settings. However, experiments in [6, 31] along with the recent success of Monte Carlo methods in [44] hint that LSTD policy iteration might have certain weakness, though no theoretical explanation is provided. The existence of this weakness is also supported by the experimental results in this paper (i.e., our algorithm outperforms existing LSTD policy iteration algorithms [20, 54] without increased com-

putational complexity), though once again no theoretical explanation is offered for the difference in results.

Outside of this paper IRL has been applied to a number of problems: human to computer behavior transfer [2, 16, 19, 37], human behavior inference [33, 12] and human behavior prediction [56, 57, 21, 38]. To the best of the author’s knowledge this paper is the first experiment using IRL for an FI.

Regarding FI’s, existing research suggests these operate primarily through information [48, 52], attention [52, 18] and motivation [52, 18] processes. Additionally, FI’s have been shown to, in general, have highly variable outcomes [18, 14]. There is no reason to believe any of these observations should be different for the experiment reported below.

In application, FI’s have been studied for human behavior change [15, 22, 9], academic learning [43, 42] and motor skill acquisition [51, 26, 29, 30]. This paper is unique from previous studies in its use of IRL to learn a complex FI signal from human examples rather than having a researcher design one by hand.

3. Preliminaries

The primary mathematical model used in both RL and IRL is known as a discounted *Markov decision process* (MDP). Informally, a discounted MDP is a stochastic model that describes goal directed agents and the environment they are acting within.

Formally, here a discounted MDP is a tuple $(S, A, \mathcal{P}, d, \pi, R, \gamma)$ where S is a finite set of states, A is a finite set of actions, $\mathcal{P} = \{p_{(s,a)} : S \rightarrow [0, 1] \mid (s, a) \in S \times A\}$ is a family of probability mass functions (with $p_{(s,a)}(s')$ being the probability of a transition from state s to state s' after action a), $d : S \rightarrow [0, 1]$ is an initial state probability mass function, the policy $\pi : A \times S \rightarrow [0, 1]$ is the conditional probability of taking action a in state s , $R : S \rightarrow \mathbb{R}$ is a reward function, and $\gamma \in [0, 1)$ is the discount factor.

MDP states and actions can be viewed as random variables $X_t(\omega) = s_t$ and $Y_t(\omega) = a_t$ in a stationary discrete Markov stochastic process $(X_t(\omega), Y_t(\omega)) = (s_t, a_t) = \omega_t$, $\omega \in (S \times A)^T$ with

$$\Pr_{(d,\pi)}(\omega) = d(s_1)\pi(a_1, s_1) \prod_{t=1}^{T-1} p_{(s_t, a_t)}(s_{t+1})\pi(a_{t+1}, s_{t+1}).$$

The expectation for this process is defined as $\mathbb{E}_d^\pi[f] = \sum_\omega f(\omega)\Pr_{(d,\pi)}(\omega)$. To simplify notation define \mathbb{E}_s^π to be the special case of \mathbb{E}_d^π where $d(s) = 1$. If the policy evolves based on past history, using π_t for π at time t , the sequence (π_1, π_2, \dots) is called a history dependent randomized policy.

In the RL problem formulation R is known and an optimal policy π^* needs to be learned. Policies are evaluated in terms of their value with respect to R ,

$$V_R^\pi(s) = \mathbb{E}_s^\pi \left[\sum_{t=1}^T \gamma^{t-1} R(X_t) \right].$$

with a (d, ϵ) -optimal policy π^* (cf. [7, 45]), for $\epsilon > 0$, being any policy satisfying

$$\mathbb{E}_d^{\pi^*} \left[\sum_{t=1}^T \gamma^{t-1} R(X_t) \right] \geq \max_{\pi} \mathbb{E}_d^{\pi} \left[\sum_{t=1}^T \gamma^{t-1} R(X_t) \right] - \epsilon.$$

In the IRL problem formulation π^* is known and a reward function making π^* optimal needs to be learned. This condition is expressed as find $R : S \rightarrow \mathbb{R}$ such that

$$\mathbb{E}_s^{\pi^*} \left[\sum_{t=1}^T \gamma^{t-1} R(X_t) \right] \geq \mathbb{E}_s^{\pi} \left[\sum_{t=1}^T \gamma^{t-1} R(X_t) \right] \quad \forall \pi \quad \forall s.$$

Unfortunately, the above condition is known to have degenerate solutions (e.g., $R = \mathbf{0}$). To deal with this, IRL algorithms introduce constraints to make sure a useful solution is generated. Additionally, perfect knowledge of π^* is often not possible. Therefore most IRL algorithms simply require access to observations of an expert whose policy π_E is *assumed* optimal with respect to the unknown R .

4. Algorithms

The two algorithms developed for this study are now introduced. New algorithms were developed due to existing algorithms either being too slow for the designed MDP, in the case of IRL (see Section 4.2), or producing sub-par policies given a reward, in the case of RL (see Section 4.4). Additionally, as briefly mentioned above, both an IRL and RL were needed due to the IRL algorithm requiring solutions to an RL problem on each iteration.

4.1. Kernel Projection IRL Algorithm

Kernel projection IRL (KPIRL) is a kernel-based extension to the well-known *projection IRL* algorithm (PIRL) [1]. Within the extension PIRL becomes the special case where the kernel is the dot product. Conditions are provided under which the more general KPIRL formulation maintains two important PIRL guarantees: (1) converging to a (d, ϵ) -optimal policy with respect to the unknown expert reward function and (2) converging within a finite number of iterations.

4.1.1. PIRL

To begin, a function mapping each MDP state to a real valued vector is defined as

$$\phi : S \rightarrow \mathbb{R}^k. \tag{1}$$

The appropriate mapping for this function is arbitrary and chosen for the problem at hand (see Section 5.4.3 for the mapping used in the human behavior experiments). Using Equation 1 a value called *feature expectation* can then be defined for some T as

$$\mu_{\phi}(\pi) = \mathbb{E}_d^{\pi} \left[\sum_{t=1}^T \gamma^{t-1} \phi(X_t) \right]. \tag{2}$$

Combining this with a reward R_w that is linear in terms of weights w with features ϕ ,

$$R_w(s) = w^\top \phi(s), \quad (3)$$

it becomes possible to express the expected value for any d , R_w and π as

$$\bar{V}_{R_w}^\pi = \mathbb{E}_d^\pi \left[\sum_{t=1}^T \gamma^{t-1} w^\top \phi(X_t) \right] = w^\top \mu_\phi(\pi).$$

By constraining w to $\|w\|_2 \leq 1$ it can be shown, without loss of generality, that

$$|\bar{V}_{R_w}^{\pi_1} - \bar{V}_{R_w}^{\pi_2}| \leq \|\mu_\phi(\pi_1) - \mu_\phi(\pi_2)\|_2 \quad \forall \pi_1, \pi_2,$$

demonstrating that $\|\mu_\phi(\pi_E) - \mu_\phi(\pi)\|_2 \leq \epsilon$ is a sufficient condition for π to be (d, ϵ) -optimal on the unknown expert reward function R_E (assuming π_E is an optimal policy for R_E and that R_E can be represented by Equation 3). Because of this the PIRL algorithm creates a sequence of policies $\bar{\pi}_i$ which converge to $\lim_{i \rightarrow \infty} \mu_\phi(\bar{\pi}_i) = \mu_\phi(\pi_E)$.

To create the sequence $\bar{\pi}_i$ PIRL first estimates $\mu_\phi(\pi_E)$ with M samples from $\Pr_{(d, \pi_E)}$,

$$\hat{\mu}_\phi(\pi_E) = \frac{1}{M} \sum_{m=1}^M \sum_{t=1}^T \gamma^{t-1} \phi(X_t(\omega_m)). \quad (4)$$

Using this estimate to inform its search PIRL iteratively generates reward function weights w_i and solves for the optimal policy π_i^* of R_{w_i} until the set of solved policies up to iteration i , Π_i , satisfies

$$\exists \bar{\pi}_i \in \text{Conv}(\Pi_i) \text{ s.t. } \|\hat{\mu}_\phi(\pi_E) - \hat{\mu}_\phi(\bar{\pi}_i)\|_2 \leq \epsilon, \quad (5)$$

where $\text{Conv}(\Pi_i)$ is the space of policies that, at the start of an episode, samples a $\pi \in \Pi_i$ with probability equal to π 's convex weight and then follows π for the entire episode (cf. *mixed strategy* and *behavioral strategy* in [5]).

4.1.2. KPIRL

To extend PIRL to a kernel-based formulation we require the image of ϕ over S to be finite (i.e., $|\phi(S)| = N < \infty$). This allows ϕ , without loss of generality, to be defined as

$$\phi(s) = \Phi \hat{e}(s), \quad (6)$$

where $\Phi = [\phi_1 \ \phi_2 \ \dots \ \phi_N]$ and $\hat{e}(s) = e_n$, the n th standard basis vector for \mathbb{R}^N , when $\phi(s) = \phi_n$. The introduction of \hat{e} allows *state-visitation expectation* to be defined as

$$\mu_{\hat{e}}(\pi) = \mathbb{E}_d^\pi \left[\sum_{t=1}^T \gamma^{t-1} \hat{e}(X_t) \right]. \quad (7)$$

Combining this with a kernel-based reward R_α , for which $\alpha \in \mathbb{R}^N$ is a weight vector,

$$R_\alpha(s) = \alpha^\top \mathbf{K}(\Phi, \Phi) \hat{e}(s) \quad (8)$$

and $\mathbf{K}(\Phi, \Phi) \in \mathbb{R}^{N \times N}$ with $\mathbf{K}_{ij}(\Phi, \Phi) = k(\phi_i, \phi_j)$ given some $k : \phi(S) \times \phi(S) \rightarrow \mathbb{R}$, it becomes possible to represent the expected value for any d , R_α and π as

$$\bar{V}_{R_\alpha}^\pi = \mathbb{E}_d^\pi \left[\sum_{t=1}^T \gamma^{t-1} \alpha^\top \mathbf{K}(\Phi, \Phi) \hat{e}(X_t) \right] = \alpha^\top \mathbf{K}(\Phi, \Phi) \mu_{\hat{e}}(\pi). \quad (9)$$

It can be shown for $\bar{V}_{R_\alpha}^\pi$, with appropriate classes of k (considered later in the paper),

$$|\bar{V}_{R_\alpha}^{\pi_1} - \bar{V}_{R_\alpha}^{\pi_2}| \leq \|\mu_{\hat{e}}(\pi_1) - \mu_{\hat{e}}(\pi_2)\|_{2,k},$$

where $\|x\|_{2,k}^2 = x^\top \mathbf{K}(\Phi, \Phi) x$. This result, combined with an empirical estimate $\hat{\mu}_{\hat{e}}$ attainable similar to Equation 4, implies that a (d, ϵ) -optimal policy, within some margin of error around the estimates, has been generated by KPIRL when

$$\exists \bar{\pi}_i \in \text{Conv}(\Pi_i) \text{ s.t. } \|\hat{\mu}_{\hat{e}}(\pi_E) - \hat{\mu}_{\hat{e}}(\bar{\pi}_i)\|_{2,k} \leq \epsilon. \quad (10)$$

An important question that has been left unanswered is what forms of k are admissible if Equation 10 is to be sufficient for the (d, ϵ) -optimality of $\bar{\pi}_i$. It is claimed that one answer is the class of positive definite kernels (i.e., any k that induces a positive semi-definite matrix \mathbf{K}).

To prove the above claim the work in [3] is built upon, where it is shown that for any positive definite kernel there exists a unique Hilbert space H of functions $\mathbb{R}^{\phi(S)}$ for which k is a reproducing kernel. That is, $f(\phi) = \langle f, k(\phi, \cdot) \rangle \forall f \in H$ and $k(\phi(S), \cdot) \subseteq H$.

Given that k is a reproducing kernel for H Equation 9 can be expressed as an inner product in this space. That is, $\bar{V}_{R_\alpha}^\pi = \langle \bar{V}_{R_\alpha}, \bar{V}_\pi \rangle$ where $\bar{V}_{R_\alpha} = \sum_{i=1}^N \alpha_i k(\phi_i, \cdot)$ and $\bar{V}_\pi = \sum_{i=1}^N (\mu_{\hat{e}}(\pi))_i k(\phi_i, \cdot)$. Using this formulation and the constraint $\|\alpha\|_{2,k} \leq 1$

$$\begin{aligned} |\bar{V}_{R_\alpha}^{\pi_E} - \bar{V}_{R_\alpha}^\pi| &= |\langle \bar{V}_{R_\alpha}, \bar{V}_{\pi_E} \rangle - \langle \bar{V}_{R_\alpha}, \bar{V}_\pi \rangle| \\ &= |\langle \bar{V}_{R_\alpha}, \bar{V}_{\pi_E} - \bar{V}_\pi \rangle| \\ &\leq \|\bar{V}_{R_\alpha}\|_2 \|\bar{V}_{\pi_E} - \bar{V}_\pi\|_2 \\ &= \|\alpha\|_{2,k} \|\mu_{\hat{e}}(\pi_E) - \mu_{\hat{e}}(\pi)\|_{2,k} \\ &\leq \|\hat{\mu}_{\hat{e}}(\pi_E) - \hat{\mu}_{\hat{e}}(\pi)\|_{2,k}, \end{aligned}$$

proving that Equation 10 is sufficient to show (d, ϵ) -optimality of any π on R_E .

Finally, it remains to be shown under which conditions KPIRL maintains PIRL's guarantee of convergence in finite iterations. The proof in [1] shows that PIRL's convergence rate is a function of R_w 's dimension. Because Hilbert spaces can have infinite dimensions it might seem that convergence is no longer guaranteed. Fortunately this is not the case as KPIRL only has to search within the linear span of $k(\phi(S), \cdot)$ to find an optimal solution (cf. *the representer theorem* [41]). This span has dimension of at most N (as required above), and thus PIRL's proof of convergence rate in finite iterations is preserved.

The full KPIRL algorithm is provided in Algorithm 1. Further justification for the algorithm's iterative search method, as well as the proofs of convergence in finite time,

are left to [1].

Algorithm 1 Kernel Projection IRL (KPIRL)

- 1: **Initialize:** set ϵ as desired according to Equation 5
 - 2: **Initialize:** set $i \leftarrow 1$ and $\mu_E \leftarrow \hat{\mu}_{\hat{e}}(\pi_E)$
 - 3: **Initialize:** set R_1 to a random reward
 - 4: **Initialize:** set $\pi_1^* \leftarrow \pi^*$ for R_1 and $\bar{\mu}_1 \leftarrow \hat{\mu}_{\hat{e}}(\pi_1^*)$

 - 5: **while** $\|\mu_E - \bar{\mu}_i\|_{2,k} > \epsilon$ **do**
 - 6: $i \leftarrow i + 1$
 - 7: $\alpha_i \leftarrow \mu_E - \bar{\mu}_{(i-1)}$
 - 8: $R_i \leftarrow \alpha_i^\top K(\Phi, \Phi) \hat{e}$
 - 9: $\pi_i^* \leftarrow \pi^*$ for R_i ▷ see Algorithm 2
 - 10: $\mu_i \leftarrow \hat{\mu}_{\hat{e}}(\pi_i^*)$
 - 11: $\kappa_i \leftarrow \frac{(\mu_i - \bar{\mu}_{(i-1)})^\top K(\Phi, \Phi) (\mu_E - \bar{\mu}_{(i-1)})}{(\mu_i - \bar{\mu}_{(i-1)})^\top K(\Phi, \Phi) (\mu_i - \bar{\mu}_{(i-1)})}$
 - 12: $\bar{\mu}_i \leftarrow \bar{\mu}_{(i-1)} + \kappa_i (\mu_i - \bar{\mu}_{(i-1)})$
 - 13: **end while**
-

4.2. Kernel Projection Benchmarks

Among existing nonlinear IRL algorithms there are two notable standouts: [25] which models the reward function as a Gaussian process and [10] which constructs features to find the best linear fit. Many IRL papers benchmark against GPIRL [25] (including [10] where GPIRL is still quite competitive), so we choose to benchmark against it as well (along with PIRL [1] for reference).

The human subjects experiments are described fully in Section 5. Here, for benchmarking purposes, simple random gridworld environments are created using the IRL Toolkit [24], an open-source MATLAB environment created for IRL research. To make sure reported metrics weren't due to chance each metric was calculated over many random gridworlds, and their mean performance was compared.

All gridworlds have $|S| = n^2$ for some $n \in \mathbb{N}$ with five actions (up, down, left, right and stay) in each state. State-action transition probabilities $p_{(s,a)}$ are deterministic, and features ϕ are assigned to states so that a nonlinear relationship exists between a state's features $\phi(s)$ and its reward value $R(s)$.

The performance of each algorithm is measured in terms of the percent of optimal value captured by the learned reward, which we call accuracy since it is a measure of how close we were to an optimal reward, and the total runtime in seconds, which we call efficiency. Figure 1 shows one of the randomly generated gridworlds and the rewards learned by the selected IRL algorithms.

In terms of accuracy, no matter the size of the state space or the number of expert trajectories, GPIRL always performed best (see Figure 2). KPIRL came in a close second, typically about 5% behind GPIRL. The linear algorithm, PIRL, performed worst (which was expected since the features and reward were constructed to have a nonlinear relationship).

In terms of efficiency, KPIRL and PIRL are the clear winners (see Figure 3). The runtime for both remained near zero for all state space sizes $|S|$ and expert trajectory counts M (see Equation 4) while GPIRL runtime grew exponentially.

In the end, when dealing with large amounts of data and large state spaces, KPIRL

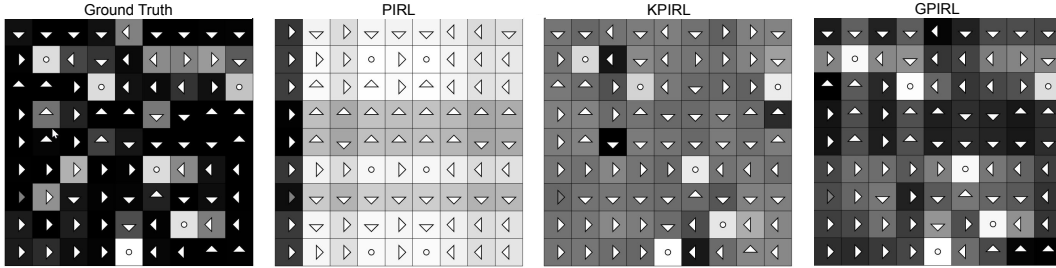


Figure 1. These four figures compare the output of one run of PIRL, KPIRL and GPIRL to Ground Truth. The leftmost grid is the expert’s reward and policy. The right three grids show the rewards learned by PIRL, KPIRL and GPIRL (respectively) after observing the expert. A state’s reward value is indicated by its shading, with white indicating high reward and black indicating low reward. The arrows indicate the optimal action for each state when following the displayed reward.

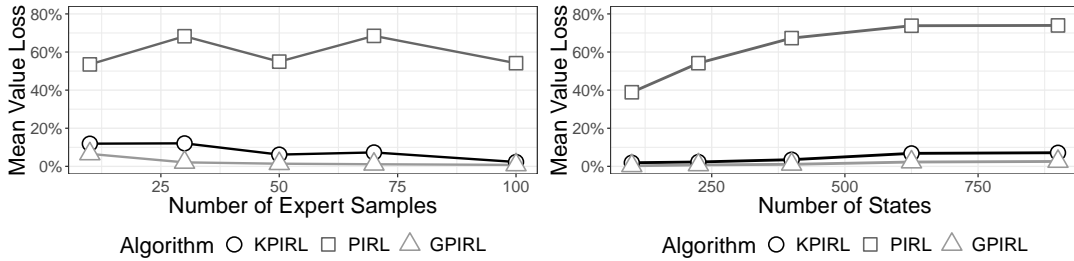


Figure 2. Both figures show the average percent of value lost when the optimal policy for the IRL reward is compared to the true expert policy. The lower the percentage loss the better the IRL reward. On the left performance is plotted as a function of the expert trajectory samples. On the right performance is plotted as a function of the MDP’s number of states.

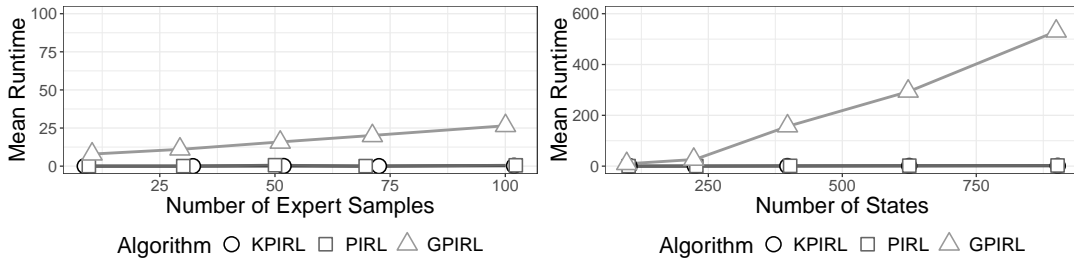


Figure 3. On the left is the mean time to convergence for KPIRL, PIRL and GPIRL as a function of the number of expert trajectories. On the right is the mean time to convergence as a function of the number of states in the MDP. The times reported in both figures are in seconds.

seems to be the better algorithm. It sacrifices a small amount accuracy for large gains in efficiency. On the other hand, when accuracy is most important, the state space is relatively small and there are few expert examples GPIRL seemed the better algorithm.

4.3. Kernel Lookup Algorithm

Kernel lookup approximation (KLA) is a model-free, on-policy, Monte Carlo, approximate RL algorithm. KLA requires either direct or simulated interaction with an environment along with a reward signal for every visited state (as opposed to intermittent reward signals).

4.3.1. Improving The Policy

The primary algorithmic strategy used in KLA is *generalized policy iteration* (GPI) [46] via iterative improvements to a Q-function [50]. This high-level procedure is provided in Algorithm 2.

One unique aspect of the KLA algorithm which can be seen at this level is the pairing of a traditional lookup function \dot{Q} (cf. [49]) with an approximate function \bar{Q} (cf. [20, 54]). Maintaining both functions separately allows for optimal updates (see Section 4.3.3) and confidence estimates (see Section 4.3.2) while still generalizing to unseen states.

In addition to maintaining two Q-functions KLA also formulates these functions as members of $\mathcal{P} \rightarrow \mathbb{R}$ (cf. *post-decision states* [34]) rather than $S \times A \rightarrow \mathbb{R}$ (cf. *action-values* [50]). This change in formulation loses no information since

$$p_{(s,a)} = p_{(s',a')} \implies Q(s, a) = Q(s', a'), \forall (s, a), (s', a') \in S \times A$$

while at the same time potentially reducing the dimension of Q due to $|\mathcal{P}| \leq |S \times A|$.

Finally, because there are two Q-functions, it should be noted that the greedy policy being improved in KLA is with respect to \bar{Q} rather than \dot{Q} . To make this distinction clear in the KLA discussions below this policy will be denoted

$$\bar{\pi}_n(a, s) = \begin{cases} 1, & \text{if } a = \operatorname{argmax}_{a \in A} \bar{Q}_n(p_{(s,a)}) \\ 0, & \text{otherwise} \end{cases}.$$

Algorithm 2 Kernel Lookup Approximation

- 1: **Initialize:** set N to the desired number of policy iterations
- 2: **Initialize:** set $\dot{Q}_0 \leftarrow \mathbf{0}$, the lookup Q-function
- 3: **Initialize:** set $\bar{Q}_0 \leftarrow \mathbf{0}$, the general Q-function

Step 1: Iterate N times on \bar{Q}

- 4: **for** $n \leftarrow 1$ to N **do**
 - 5: $O_n \leftarrow \text{Observe-Q-Values}(\bar{Q}_{n-1})$ ▷ Algorithm 3
 - 6: $\dot{Q}_n \leftarrow \text{Estimate-Q-Values}(\dot{Q}_{n-1}, O_n)$ ▷ Algorithm 5
 - 7: $\bar{Q}_n \leftarrow \text{Generalize-Q-Values}(\bar{Q}_n)$ ▷ Algorithm 6
 - 8: **end for**
 - 9: **Return:** $\bar{\pi}_N(a, s)$
-

4.3.2. Observing Q-Values

On each iteration n KLA requires an observation set $O_n \subseteq \mathcal{P} \times \mathbb{R}$ to move \dot{Q}_{n-1} closer to $Q^{\bar{\pi}_{n-1}}$. Generating observations requires manually specifying the episode count $M \in \mathbb{N}$, episode length $T \in \mathbb{N}$ and observations per episode $W \in \mathbb{N}$. Using M, T, W, d and $\bar{\pi}_{n-1}$ an episode collection can be constructed and fixed as

$$E_n \leftarrow \{\omega_m \sim \Pr_{(d, \bar{\pi}_{n-1})} \mid |\omega_m| = T + W, m = 1, 2, \dots, M\}, \quad (11)$$

from which O_n can be constructed via

$$O_n \leftarrow \left\{ \left(p_{(X_w, Y_w)}, \sum_{t=1}^T \gamma^{t-1} R(X_{(t+w)}) \right) \mid (\omega, w) \in E_n \times \{1, 2, \dots, W\} \right\}.$$

Episodes generated according to Equation 11 will only exploit \bar{Q}_{n-1} . To improve on this KLA uses an exploration heuristic to select the first action in an episode according to an upper bound estimate. This upper bound is estimated from quantities generated by Algorithm 4 (i.e., $\text{Var}(\dot{Q}_{n-1}(p)) \approx \lambda_p \bar{\sigma}_p^2$ and $\text{Bias}(\dot{Q}_{n-1}(p)) \approx \beta_p$), and the estimate is only used when enough observations of p have been collected for some measure of confidence (i.e., $c_p \geq 3$).

Algorithm 3 KLA Observing Q-Values Subroutine

- 1: **Initialize:** set M, T and W for episodes, steps and observations/episode
- 2: **Inputs:** \bar{Q}_{n-1} , the generalized Q-function from Algorithm 2
- 3: **Requires:** $c, \lambda, \bar{\beta}$ and $\bar{\sigma}^2$ from Algorithm 4

Step 1: Define the upper bound heuristic functions

- 4: $U(p) := 2\sqrt{\lambda_p \bar{\sigma}_p^2} + \bar{\beta}_p$
- 5: $E(p) := \begin{cases} U(p), & \text{if } c_p \geq 3 \\ \max_{\{p \in \mathcal{P} \mid c_p \geq 3\}} U(p), & \text{otherwise} \end{cases}$

Step 2: Generate the observation set O

- 6: $O_n \leftarrow \emptyset$
 - 7: **for** $m \leftarrow 1$ to M **do**
 - 8: $s_1 \sim d$
 - 9: $a_1 \leftarrow \operatorname{argmax}_{a \in A} [\bar{Q}_{n-1}(p_{(s_1, a)}) + E(p_{(s_1, a)})]$
 - 10: **for** $t \leftarrow 2$ to $T + W$ **do**
 - 11: $s_t \sim p_{(s_{t-1}, a_{t-1})}$
 - 12: $a_t \sim \bar{\pi}_{n-1}(A, s)$
 - 13: **end for**
 - 14: **for** $w \leftarrow 1$ to W **do**
 - 15: $O_n \leftarrow O_n \cup \{(p_{(s_w, a_w)}, \sum_{t=1}^T \gamma^{(t-1)} R(s_{(t+w)}))\}$
 - 16: **end for**
 - 17: **end for**
 - 18: **Return:** O_n
-

4.3.3. Estimating Q-Values

Q-value lookup estimates are updated with the observation set O_n from Algorithm 3. This set contains elements $(p, q_{(p,n)}) \in O_n$ where $q_{(p,n)}$ is an unbiased but noisy observation of $\dot{Q}^{\bar{\pi}_{n-1}}(p)$. With these observations the KLA update rule can generally be defined as

$$\dot{Q}_{c+1}(p) \leftarrow \dot{Q}_c(p) + (\alpha_p)_c \left((q_{(p,n)})_c - \dot{Q}_c(p) \right),$$

where c indicates the update iteration and $(\alpha_p)_c \in [0, 1]$ is a step size. When (p, n) is fixed and the observations $q_{(p,n)}$ are uniformly bounded it has been shown in [39] that the above update rule converges in probability to $\lim_{c \rightarrow \infty} \dot{Q}_c(p) = \mathbb{E}[q_{(p,n)}] = \dot{Q}^{\bar{\pi}_{n-1}}(p)$ so long as $\sum_{c=1}^{\infty} (\alpha_p)_c = \infty$ and $\sum_{c=1}^{\infty} (\alpha_p)_c^2 < \infty$.

To determine $(\alpha_p)_c$ on each iteration of c the *optimal stepsize algorithm* (OSA) from [13] is used (it should be noted that whether OSA satisfies $\sum (\alpha_p)_c^2 < \infty$ is an open question). The OSA approach determines the optimal $(\alpha_p)_c$ by solving

$$(\alpha_p)_c = \operatorname{argmin}_{\alpha} \mathbb{E} \left[\left(\dot{Q}_c(p) + \alpha \left((q_{(p,n)})_c - \dot{Q}_c(p) \right) - \dot{Q}^{\bar{\pi}_{n-1}}(p) \right)^2 \right]. \quad (12)$$

By assuming that $\operatorname{Var}(q_{(p,n)}) = \sigma_p^2$, that $\dot{Q}_c(p)$ is biased with respect to $\dot{Q}^{\bar{\pi}_{n-1}}(p)$ and that $q_{(p,n)}$ is unbiased with respect to $\dot{Q}^{\bar{\pi}_{n-1}}(p)$ the solution to Equation 12 can be written as

$$(\alpha_p)_c = 1 - \sigma_p^2 / (\delta_p)_c,$$

where $\sigma_p^2 = \operatorname{MSE}_{\dot{Q}^{\bar{\pi}_{n-1}}(p)}[q_{(p,n)}]$ and $(\delta_p)_c = \operatorname{MSE}_{\dot{Q}^{\bar{\pi}_{n-1}}(p)}[\dot{Q}_c(p)] + \operatorname{MSE}_{\dot{Q}^{\bar{\pi}_{n-1}}(p)}[q_{(p,n)}]$.

The OSA method to solve for $(\alpha_p)_c$ is provided in Algorithm 4, with full justification for the approach and assumptions left to [13]. The KLA procedure using OSA is provided in Algorithm 5. In both algorithms the c indexes, which were included above to make iterations clear, have been removed as these become cumbersome to track between policy iterations and distract from the overall algorithmic intention.

4.3.4. Generalizing Q-Values

The final step in KLA is to generalize \dot{Q} . This step is required because \dot{Q} only possesses estimates for $p \in \mathcal{P}$ that have been observed. To generalize to unobserved p the function

$$\theta : \mathcal{P} \rightarrow \mathbb{R}^k \quad (13)$$

is required, along with $\tilde{\mathcal{P}} = \{p \in \mathcal{P} \mid c_p > 0\}$ where c_p is the observation count for p in Algorithm 4. Using $\theta(\tilde{\mathcal{P}})$ and $\dot{Q}(\tilde{\mathcal{P}})$ a kernel-based support vector regressor K_n is fit and \bar{Q}_n defined so that $\bar{Q}_n(p) = K_n(\theta(p))$.

The full outline of this method is provided in Algorithm 6.

4.4. Kernel Lookup Benchmarks

To benchmark KLA 2,000 random rewards R_i were generated and fixed for the MDP defined in Section 5.4.1. With the rewards fixed the expected value for a policy iteration

Algorithm 4 Optimal Step-size Algorithm [13]

- 1: **Initialize:** set $\lambda \leftarrow \mathbf{0}$ and $c \leftarrow \mathbf{0}$ only on the first call
- 2: **Inputs:** p , $q_{(p,n)}$ and $\dot{Q}_n(p)$

Step 1: Increase observation count

- 3: $c_p \leftarrow c_p + 1$

Step 2: Calculate plug-in estimates

- 4: $\nu_p \leftarrow \begin{cases} 1, & \text{if } c_p = 1, 2 \\ \frac{\nu_p}{1+\nu_p-0.05}, & \text{otherwise} \end{cases}$
- 5:
- 6: $\bar{\beta}_p \leftarrow (1 - \nu_p)\bar{\beta}_p + \nu_p \left(q_{(p,n)} - \dot{Q}_n(p) \right)$
- 7: $\bar{\delta}_p \leftarrow (1 - \nu_p)\bar{\delta}_p + \nu_p \left(q_{(p,n)} - \dot{Q}_n(p) \right)^2$
- 8: $\bar{\sigma}_p^2 \leftarrow \frac{\bar{\delta}_p - \bar{\beta}_p^2}{1+\lambda_p}$

Step 3: Calculate step-size values

- 9: $\alpha_p \leftarrow \begin{cases} 1/c_p, & \text{if } c_p = 1, 2, 3 \text{ or } \bar{\delta}_p = 0 \\ 1 - \bar{\sigma}_p^2/\bar{\delta}_p, & \text{otherwise} \end{cases}$
 - 10: $\lambda_p \leftarrow \alpha_p^2 + (1 - \alpha_p)^2 \lambda_p$
 - 11: **Return:** α_p
-

Algorithm 5 KLA Estimate Q-Values Subroutine

- 1: **Inputs:** \dot{Q}_{n-1} and O_n from Algorithm 2

Step 1: Initialize \dot{Q}_n with \dot{Q}_{n-1}

- 2: $\dot{Q}_n \leftarrow \dot{Q}_{n-1}$

Step 2: Smooth O_n into \dot{Q}_n

- 3: **for all** $(p, q_{(p,n)}) \in O_n$ **do**
- 4: $\alpha_p \leftarrow \text{OSA}(p, q_{(p,n)}, \dot{Q}_n(p))$
- 5: $\dot{Q}_n(p) \leftarrow \dot{Q}_n(p) + \alpha_p(q_{(p,n)} - \dot{Q}_n(p))$
- 6: **end for**

- 7: **Return:** \dot{Q}_n
-

Algorithm 6 KLA Generalize Q-Values Subroutine

- 1: **Inputs:** \dot{Q}_n , the current lookup Q-values from Algorithm 2
- 2: **Requires:** θ , the feature map for the post-decision states
- 3: **Requires:** c , the observation counts from Algorithm 4

- 4: $\tilde{\mathcal{P}} \leftarrow \{p \in \mathcal{P} \mid c_p > 0\}$
- 5: $K_n \leftarrow \text{Fit-Kernel-SVM-Regressor}(\theta(\tilde{\mathcal{P}}), \dot{Q}_n(\tilde{\mathcal{P}}))$
- 6: $\bar{Q}_n(p) := K_n(\theta(p))$

- 7: **Return:** \bar{Q}_n
-

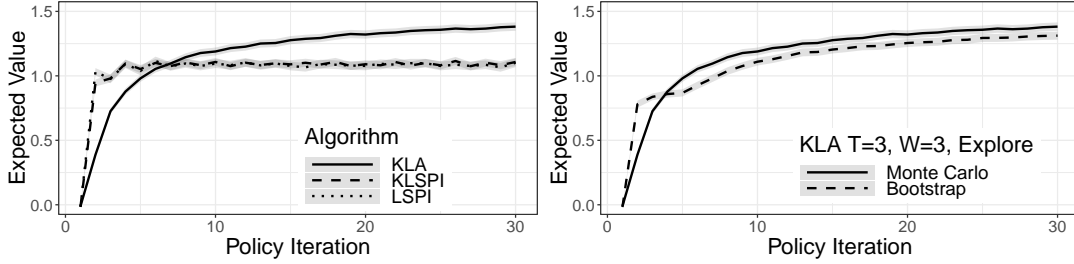


Figure 4. The left image shows a performance comparison of the average expected value per iteration for KLA, KLSPI and LSPI. Each algorithm shown has optimal parameters as described in the paper. The right image compares KLA performance based on the update target used. That is, $\sum_{t=1}^T \gamma^{(t-1)} R_t$ vs $R_t + \gamma \bar{Q}_{n-1}(p_{(s_{t+1}, a_{t+1})})$.

algorithm a across all R_i was defined as

$$f_a(n) = \frac{1}{2000} \sum_{i=1}^{2000} \mathbb{E}_d^{\pi(a,n,R_i)} \left[\sum_{t=1}^{10} .9^{(t-1)} R_i(X_t) \right],$$

where $\pi(a,n,R_i)$ represents the policy learned by algorithm a on iteration n when pursuing reward R_i . The values of this function were estimated using Monte Carlo sampling for $n = 1, 2, \dots, 30$, and the estimated results are provided in Figures 4 and 5 along with the estimate’s standard error.

The MDP and θ used to benchmark (cf. Section 5.4.1 and 5.4.3) was the same one used for the human experiments detailed in Section 5. This MDP had $|S| \approx 10^{89}$ and $|A| = 400$ along with $|\theta(\mathcal{P})| = 13,122$. The transition dynamics \mathcal{P} are detailed in Section 5.1. The initial state distribution d was a fixed, uniform distribution over a previously recorded 450 state expert trajectory (cf. Section 5.4.2).

Performance of KLA was compared to itself (across various parameters), *least-squares policy iteration* (LSPI) [20] and *kernel-based least squares policy iteration* (KLSPI) [54]. In an effort to make a fair comparison every algorithm used the same initial state distribution d , the same feature set $\theta(\mathcal{P})$ for Q-function approximation and the same number of new observations for policy evaluation on each iteration (90 episodes of length 6).

Each algorithm’s parameters were optimized via a gradient ascent search. For KLA T and W were optimized with the constraint $T + W = 6$ (optimal was $T = 3$ and $W = 3$). For LSPI the order of the polynomial basis applied to $\theta(\mathcal{P})$ was selected (optimal was the full 2nd order polynomial basis). And for KLSPI the kernel, kernel bandwidth and linear dependency pruning parameter were selected (optimal was a Gaussian kernel with a bandwidth of 1.2 and linear dependence pruned at $\mu = 0.2$).

It should also be noted that the implementation of LSPI and KLSPI solved for the projected fixed-point rather than the Bellman residual. This implementation has been shown to often be preferred [20, 11] in the case of policy iteration.

5. Experiment Setup

In what follows the two human subject experiments, which utilize the above algorithms, are described. For these experiments reward functions were learned with

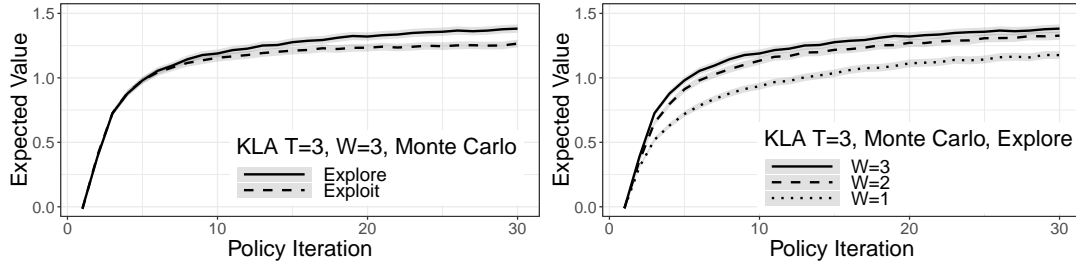


Figure 5. The left image compares the performance of KLA with the proposed upper bound exploration heuristic versus a pure exploitation strategy. The right image shows the effects of modulating the observations per episode count W .

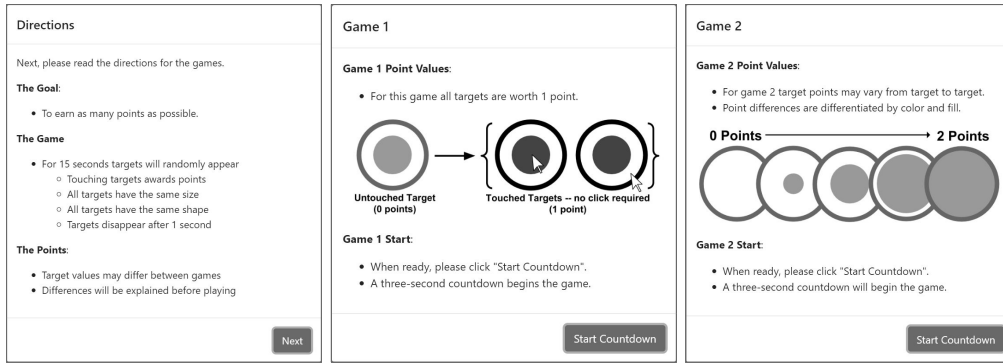


Figure 6. The three direction screens shown to experiment participants. These screens were identical for all participants, regardless of their treatment group.

KPIRL and then subsequently used as interventions to either increase or decrease performance in four treatment groups. The experimental game, four treatments and outcome variables were identical in both experiments. The only difference between experiments was a slight improvement in experimental design, strengthening the causal inference.

5.1. Experiment Game

To test the treatment effect participants were asked to play two 15 second games. Gameplay consisted of touching (no clicking required) randomly appearing targets in order to receive points. The first game was identical for all participants, regardless of their treatment group, to provide a baseline, pretest observation while the second game provided posttest observations of treatment effects.

Participants were informed before the game began that their goal was to earn as many points as possible. All participants, regardless of their treatment group, were provided with identical directions as shown in Figure 6. Direction screens were displayed to participants one at a time with directions about point values being provided just before the respective game began.

Within the game targets were always drawn as perfect circles and always had the same size relative to the area of the playing field. Targets remained on screen for one second and could be touched multiple times so long as the cursor was first removed

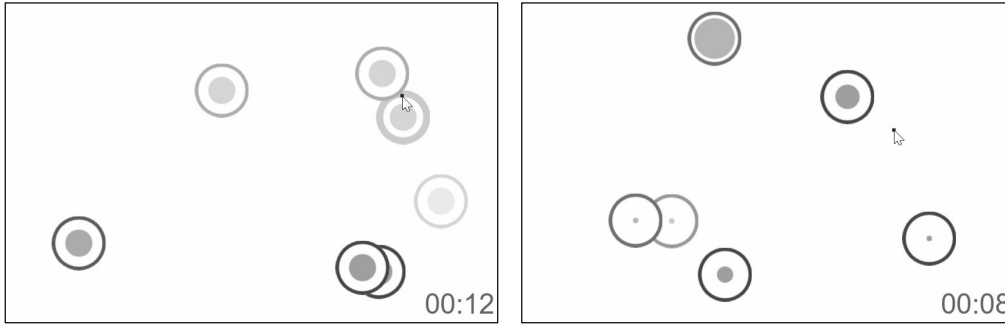


Figure 7. The left image shows a pretest game. The right image shows a posttest game with a treatment. For all games target point values were communicated via a target’s fill. The more filled in a target the more points it was worth. All games were drawn in grayscale for all participants.

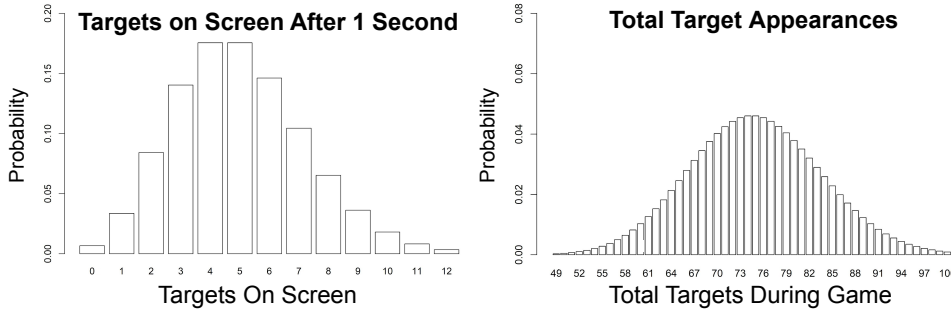


Figure 8. On the left is the distribution of the total number of targets that could be on the screen at any one time during the course of the game. On the right is the distribution of the total number of targets that could appear during the course of an entire game.

from the target. Two examples of games in progress can be seen in Figure 7.

Target point values were indicated by the amount of fill in the center of a target. Participants were told that fully filled targets were worth two points when touched while empty targets were worth zero points (cf. Figure 7 and 6). In the event that a target’s point value changed during a game (i.e., in the posttest game of a non-control group participant), updates to a target’s fill occurred at a frequency of 30Hz.

Targets appeared according to a one millisecond Poisson distribution with $\lambda = \frac{1}{200}$. This meant that after a one second warm up period there were an average of 5 targets on-screen at any one time (see left of Figure 8) with 75 targets expected to appear over the course of a full 15 second game (see right of Figure 8).

When a target did appear it was placed according to a uniform distribution over the entire area of play with the constraint that targets had to be fully within 5 pixels of the playing field boundaries. The five pixel margin prevented targets from being placed exactly on an edge where they would have had a theoretically infinite size.

To handle different screen sizes and resolutions all targets were scaled to have an area equal to 1.57% of the playing field. This scaling also handled the case of browser windows not at maximum size. With scaling, the expected number of touches for random movement, on any screen, was $71.28 \pm 0.2741SE$ (estimated via Monte Carlo simulation with a policy of uniformly random cursor movement).

To prevent potential confounding factors due to color all games were drawn with a grayscale color palette (exactly as the images in this document show). Untouched

Experiment 1 Design				Experiment 2 Design			
N	O		O	R	O		O
N	O	X ₁	O	R	O	X ₁	O
N	O	X ₂	O	R	O	X ₂	O
N	O	X ₃	O	R	O	X ₃	O
N	O	X ₄	O	R	O	X ₄	O

Figure 9. Both experiments are summarized using common experimental design notation. It can be seen that each experiment had four treatment groups, a control group, a pretest and a posttest. The only difference was in assignment. Experiment 1 had non-random assignment while Experiment 2 had random assignment (as indicated by the “N” and “R” above).

targets were drawn using a dark grey brush while touched targets were drawn with a black brush.

5.2. Experiment Design

For the experiments a pretest-posttest design was followed with a control group and four treatments. The only difference between experiment designs was the assignment protocol (as seen in Figure 9). This difference was due simply to an initial lack of experience with the online recruitment platform. The outcome variable and treatments remained unchanged between experiments.

For both experiments the outcome variable was defined to be the number of points a participant would have earned in a game had all targets been worth one point (i.e., the number of targets that a participant touched in a game). This value was referred to as a participant’s “performance.”

In a pretest game all participants’ targets (regardless of the participant’s treatment group) were drawn to indicate one point for each target. This matched the true point value with respect to the outcome variable.

In posttest games targets were drawn to indicate point values according to a participant’s treatment group. Participants in the control group had their posttest targets drawn to indicate one point for each target (i.e., the same as all pretest games). Participants in a non-control group had their targets drawn to indicate between zero and two points, according to their treatment group’s reward function. Participants were never made aware of the true “performance” metric.

In order to measure performance, observations of the 15 second games were collected with a frequency of 30Hz. This sampling rate meant that, in theory, a performance had an upper bound of 450 touches (and a lower bound of 0). In practice, no participant ever came close to the upper bound (though many hit the lower bound).

5.3. Participant Recruitment

Between both experiments 3,256 fist-time, mouse-using participants were recruited through Amazon Mechanical Turk (AMT), an online marketplace for hiring short-term “workers.” All participants were compensated for their involvement in the experiment, and compensation was not contingent upon experimental performance or completion.

Before collecting data participants were provided a voluntary consent agreement. The consent agreement (along with the entire experimental protocol) was approved by the University of Virginia’s institutional review board for social and behavior studies.

After consenting participants were asked to provide five pieces of information: (1) age range (e.g., 18-24 and 25-34), (2) gender, (3) computer type (e.g. tablet, smart-phone or laptop), (4) input device (e.g., mouse, touchpad or touchscreen) and (5) if this was their first time participating in the experiment. The specific demographics of participants are provided within the context of each experiment’s results in Section 6.

5.4. Treatment Groups

In total, four reward functions (identified as R_{HH} , R_{HL} , R_{LH} and R_{LL} and described in detail below) were learned and used as treatments in four separate treatment groups (i.e., treatment group 1 was shown reward R_{HH} , treatment group 2 was shown reward R_{HL} , etc.). To learn the reward functions for the treatment groups five steps were taken: (1) define the MDP’s S , A and \mathcal{P} , (2) find a high and low performing experts to learn reward functions from, (3) define ϕ , \hat{e} and k for KPIRL and θ for KLA, (4) learn initial reward functions using KPIRL and (5) post-process the KPIRL reward functions to aid in human interpretation.

5.4.1. Definitions of States, Actions and Transitions

For the game described above, and used in the experiment, the state set was defined

$$S = \mathcal{X} \times \mathcal{Y} \times \dot{\mathcal{X}} \times \dot{\mathcal{Y}} \times \ddot{\mathcal{X}} \times \ddot{\mathcal{Y}} \times \mathcal{W} \times \mathcal{H} \times \mathcal{T},$$

where the sets $\mathcal{X}, \mathcal{Y}, \dot{\mathcal{X}}, \dot{\mathcal{Y}}, \ddot{\mathcal{X}}, \ddot{\mathcal{Y}} \in \mathbb{Z}$ are all possible values for the cursor’s x, y position, velocity and acceleration, the sets $\mathcal{W}, \mathcal{H} \in \mathbb{Z}$ are all possible values for the playing field’s width/height in pixels and \mathcal{T} is the power set containing all subsets of possible target x -locations, y -locations, radiuses and ages.

The action set was defined $A = \dot{\mathcal{X}} \times \dot{\mathcal{Y}}$, where $\dot{\mathcal{X}}, \dot{\mathcal{Y}} \in \mathbb{Z}$ were possible changes in cursor position (e.g. $(1, 1) \in A$ would represent moving the cursor one pixel right and one pixel down). It should be noted that in practice, when solving for optimal policies in KPIRL (i.e., using KLA) the action space was truncated, for tractability, to $\tilde{A} \subset [-150, 150] \times [-150, 150] \subset A$ with $|\tilde{A}| = 400$.

Finally, given some $s = [x, y, \dot{x}, \dot{y}, \ddot{x}, \ddot{y}, w, h, \mathbf{t}] \in S$ and some $a \in A$ the transition $p_{(s,a)} \in \mathcal{P}$ was defined as follows: (1) a was added deterministically to the states x and y (and all other derivatives were updated appropriately), (2) all targets in \mathbf{t} had their ages increased by 30 milliseconds, and any targets over a second old were removed, and (3) targets appeared and were positioned in \mathbf{t} with probability as described in Section 5.1 (assuming 30ms passed during the transition).

5.4.2. Human Experts

To learn reward functions two human “experts” were selected from a pre-experiment batch of 100 candidate experts. Every candidate expert was observed twice to produce two sequences $\omega_1, \omega_2 \in (S \times A)^{450}$. The two selected experts, labeled EH and EL for expert high-performer and expert low-performer respectively, were chosen due to their performance (i.e., the number of targets they touched) and input devices (i.e., a mouse, the most common input device among candidate experts). Details for the two selected

Table 1. Descriptive statistics for the two human experts.

Expert ID	Gender	Age	Input	First	Game 1 Touches	Game 2 Touches
<i>EH</i>	Male	25-34	Mouse	Yes	64	58
<i>EL</i>	Male	25-34	Mouse	Yes	20	21

experts are provided in Table 1. No data from the 100 expert candidates were used when hypothesis testing.

5.4.3. Definitions of KPIRL and KLA objects

To use KPIRL and KLA for reward learning four objects needed to be defined: ϕ , \hat{e} , k and θ . Beginning with ϕ , the following definition was selected based on intuition:

$$\phi(s) = [1 - T(s), T(s)X_p(s), T(s)Y_p(s), T(s)V_m(s), T(s)V_d(s), T(s)A_m(s)]^\top,$$

where T indicated if a target was touched, X_p was the cursor’s x -position, Y_p was the cursor’s y -position, V_m was the magnitude of the cursor’s velocity, V_d was the direction of the cursor’s velocity and A_m was the magnitude of the cursor’s acceleration.

Considering the common heuristic technique of bias-variance trade-off in function approximation it was additionally decided to restrict the size of ϕ by mapping the features to larger bins. Given $s = [x, y, \dot{x}, \dot{y}, \ddot{x}, \ddot{y}, w, h, \mathbf{t}] \in S$ the exact binned definitions can be written

$$\begin{aligned} X_p(s) &= \min\left(2, \left\lfloor 3 \left(\frac{x}{w}\right) \right\rfloor\right) & V_m(s) &= \min\left(7, \left\lfloor 8 \left(\frac{\|\dot{x}, \dot{y}\|}{48}\right) \right\rfloor\right) \\ Y_p(s) &= \min\left(2, \left\lfloor 3 \left(\frac{y}{h}\right) \right\rfloor\right) & A_m(s) &= \min\left(5, \left\lfloor 6 \left(\frac{\|\ddot{x}, \ddot{y}\|}{60}\right) \right\rfloor\right) \\ T(s) &= \begin{cases} 1, & \text{if target in } \mathbf{t} \text{ touched} \\ 0, & \text{otherwise} \end{cases} & V_d(s) &= \min\left(7, \left\lfloor 8 \left(\frac{\text{atan2}(-\dot{y}, -\dot{x}) + \pi}{2\pi}\right) \right\rfloor\right). \end{aligned}$$

Next \hat{e} needed to be defined for KPIRL. Because of the above binning scheme it was easy to define a linear map $n : \mathbb{Z}^6 \rightarrow \mathbb{Z}$ such that $n(\phi(S)) = [1, |\phi(S)|]$. Using this map it was possible to define $\hat{e}(s) = e_{n(\phi(s))}$, the n th standard basis vector for $\mathbb{R}^{|\phi(S)|}$.

Third, KPIRL required that a positive definite kernel k be selected. In the experiment a Gaussian kernel with a bandwidth of .6 was used (the bandwidth was selected by trial and error). In addition to the bandwidth two other pieces of structure were added to k . First, k modified the velocity direction V_d to be circular since its value represented radians around a circle. And second, k modified all $\phi(S)$ so that the single “no-touch” state feature vector (i.e., $[100000]^\top$) was equidistant from every touch state feature vector (the structural modifications detailed here were also applied in the KLA benchmark for LSPI and KLSPI).

Finally, for the reported experiments, because KLA was used in conjunction with KPIRL to determine π_i^* on each KPIRL iteration, one final object was defined for KLA: θ (cf. Equation 13). The definition used in the experiments is as follows, given $s = [x, y, \dot{x}, \dot{y}, \ddot{x}, \ddot{y}, w, h, \mathbf{t}]^\top$, $a = [x', y']^\top$ and $s' = [x', y', \dot{x}', \dot{y}', \ddot{x}', \ddot{y}', w', h', \mathbf{t}']^\top \sim p_{(s,a)}$

$$\theta(p_{(s,a)}) = [x', y', \dot{x}', \dot{y}', \ddot{x}', \ddot{y}', T_a(s, a), T_e(s, a), T_s(s, a), T_1(s, a)]^\top,$$

where T_a was the number of targets being approached, T_e was an indicator that a

Table 2. The four rewards used as treatments in the experiment and their optimal policy summary.

Reward ID	Expert ID	Optimal Policy	Policy Kinematics	Policy Performance
R_{HH}	EH	π_{HH}	Similar to EH	Similar to EH
R_{HL}	EH	π_{HL}	Similar to EH	Worse than EH
R_{LH}	EL	π_{LH}	Similar to EL	Better than EL
R_{LL}	EL	π_{LL}	Similar to EL	Similar to EL

Table 3. The feature expectations (i.e., Equation 2 with $T = 10$, $\gamma = .9$ and ϕ as defined in Section 5.4.3) for optimal computer behavior (π_{CT}), human expert behavior (π_{EH} and π_{EL}) and computer behavior learned from the human experts via IRL (π_{HH} , π_{HL} , π_{LH} and π_{LL}).

Policy	T X _p	T Y _p	T V _m	T V _d	T A _m	1 - T
π_{CT}	0.0132	1.5261	1.3745	-2.8490	1.3078	16.9471
π_{EH}	2.0093	1.4241	1.1993	-0.6871	0.6614	22.4824
π_{HH}	2.6119	2.0059	1.3469	1.9244	1.1690	18.9064
π_{HL}	2.4042	1.8073	1.2613	-1.1199	0.6936	25.2415
π_{EL}	1.7452	1.1804	0.7979	2.2178	0.4558	24.8904
π_{LH}	2.6265	1.7592	1.3417	-1.4283	1.2178	19.4081
π_{LL}	1.7136	2.5636	1.1956	-1.1634	0.6215	25.5276

target was entered, T_s was an indicator that a target was neither entered nor left and T_l was an indicator that a target was left. Additionally, similar to the reward features, the above definition θ was binned in practice such that $|\theta(\mathcal{P})| = 13, 122$.

5.4.4. Generate KPIRL Reward Functions

Four reward functions were learned via KPIRL for the experiments – two functions each from the two human experts. For the high-performing expert the rewards were labeled R_{HH} and R_{HL} for high-performer high-touch and high-performer low-touch. For the low-performing expert the rewards were labeled R_{LH} and R_{LL} for low-performer high-touch and low-performer low-touch. For these labels touch referred to the performance of a computer agent seeking the reward relative to the human expert (cf. column “1 - T” in Table 3). A high-level summary of the reward functions is provided in Table 2.

Two functions were learned for each expert because KPIRL generates a stochastic set of reward functions every run. Rather than trying to pick a single best reward across all KPIRL runs the decision was made to test several rewards in the hope of learning more about how these functions might influence human behavior. To determine a single reward function from KPIRL’s set of reward functions the function whose optimal policy had a feature expectation (cf. Table 3) closest to the human expert was selected.

5.4.5. Post-Process KPIRL Reward Functions

Because the KPIRL learned reward functions were finite and discrete it was possible to calculate the reward values for all $\phi(S)$ where $|\phi(S)| = 3, 456$ (i.e., $\alpha^\top \mathbf{K}(\Phi, \Phi) I_{|\phi(S)|}$ for each reward’s α). The histogram for the values of R_{LL} and R_{HH} are provided in Figure 10.

For the authors these raw values were difficult to immediately interpret. Assuming study participants would have similar difficulties two static transformations and one dynamic transformation were made to the reward values in an effort to increase interpretability. These transformations helped satisfy one of KPIRL’s core assumptions – a learned reward function must be followed rationally if it is to result in the desired behavior.

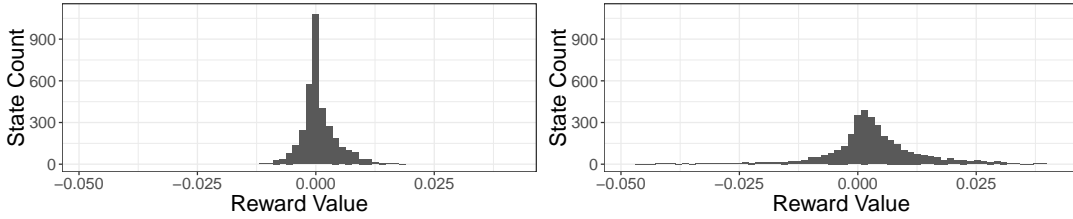


Figure 10. On the left is the histogram of reward values in R_{LL} (a reward function learned from a low-performing human expert). On the right is the same histogram but for R_{HH} (a reward function learned from a high-performing human expert).

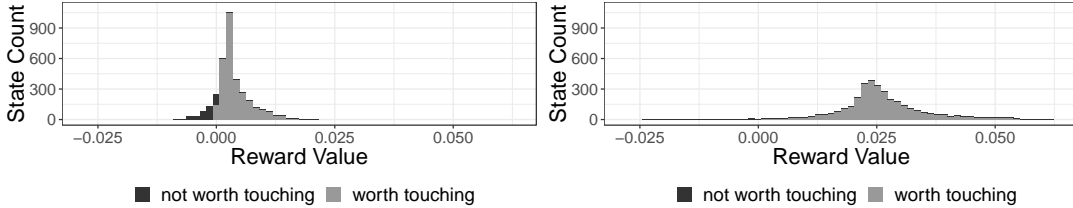


Figure 11. The reward values for R_{LL} (left) and R_{HH} (right) after shifting so that the reward value for no touch is 0. With this shift touch rewards below 0 can be interpreted as not worth touching since a participant would lose points.

The first static transformation aimed to make it more clear in absolute terms which rewards values were truly worth pursuing. To do this a structural component of the reward features was leveraged: every MDP state where no target was touched had an identical reward feature vector $\phi = [1\ 0\ 0\ 0\ 0]^T$.

This single “no-touch” reward vector was interpreted as a minimum threshold to act since a target was only worth touching if it offered more reward than not touching it. To make this threshold clear a translation was applied so that the “no-touch” reward was equal to 0 (see Figure 11).

The second static transformation aimed to encourage rational behavior by removing loss aversion [47] and reducing positive outliers. To do this reward values below 0 were clipped to 0 (i.e., avoid loss-aversion) and reward values greater than 0 were clipped at the 97th percentile (i.e., reducing outliers). The clipped distributions are shown in Figure 12.

Finally, a dynamic transformation was also applied to rewards during the course of a game. To explain this consider some target with a displayed reward of \bar{R}_t at time t .

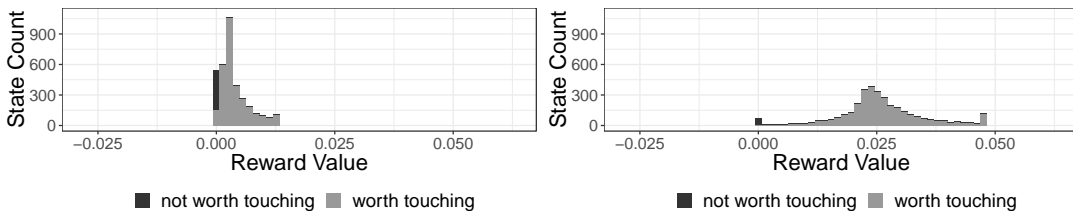


Figure 12. The reward values for R_{LL} (left) and R_{HH} (right) after shifting and clipping for interpretability.

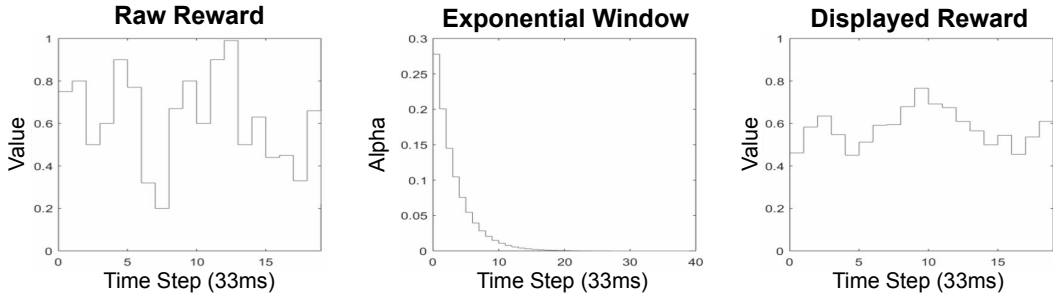


Figure 13. This figure demonstrates the effect of exponential smoothing on the displayed reward value. The figure on the left is an example of the instantaneous value R_t returned by a reward function for some target. In the middle is $\alpha = 5/18$ plotted as an exponential decay function. On the right is the final smoothed value, \bar{R}_t , which would have been displayed to participants in-game.

At the next time step this target would have a new instantaneous reward value R_{t+1} . To determine the next display value \bar{R}_{t+1} , the value R_{t+1} would be smoothed with \bar{R}_t to prevent large and sudden changes in display values. That is, $\bar{R}_{t+1} = \bar{R}_t + \alpha(R_{t+1} - \bar{R}_t)$ with $\alpha = \frac{5}{18}$. This smoothing value was selected for the value that felt most understandable through trial and error. An example of this smoothing is provided in Figure 13.

6. Experiment Results

The results of the two experiments described in Section 5 support the conjecture that IRL reward feedback can predictably increase or decrease performance. Both experiments found that increase treatments had a statistically significant effect and that only the decrease treatment had a negative effect size.

6.1. Experiment 1

6.1.1. Hypothesis

- H1₀** Feedback from a high performer’s reward function learned with KPIRL will not alter performance for first-time participants using a mouse
- H1_a** Feedback from a high performer’s reward function learned with KPIRL will increase performance for first-time participants using a mouse
- H2₀** Feedback from a low performer’s reward function learned with KPIRL will not alter performance for first-time participants using a mouse
- H2_a** Feedback from a low performer’s reward function learned with KPIRL will decrease performance for first-time participants using a mouse

6.1.2. Recruitment

To recruit participants seven separate AMT work request batches (cf. Figure 16) were posted using the data in Table 4. Separate batches were used simply because of inexperience with the platform. For each batch a work request would have appeared on participants’ devices as one option to complete among many potential requests.

Table 4. These were the attributes included with all Experiment 1 AMT work requests.

Title	Play two, quick (15 second) cursor (finger) touch games
Description	Navigate to website to complete two 15 second cursor (touch) games.
Payment	\$0.20

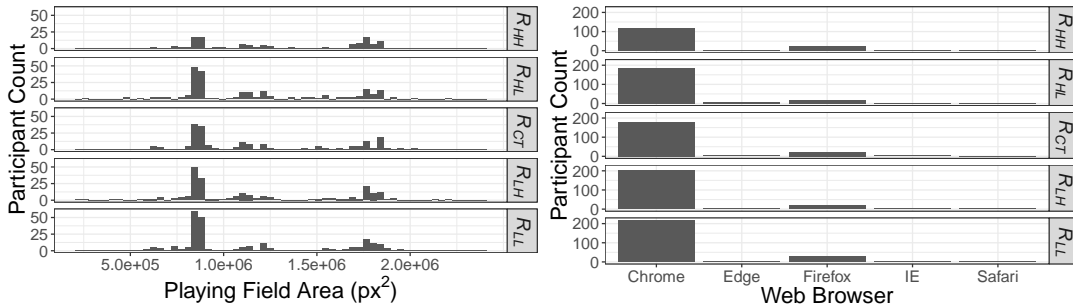


Figure 14. The browser and resolution distributions of participants by treatment group in Experiment 1.

Because participants could have participated in several batches, all participants were asked if they had participated previously before beginning. In total $n = 2,257$ participants were recruited for Experiment 1.

6.1.3. Assignment

Participants were assigned to a treatment group according to the batch they were recruited in. Because each recruitment batch occurred at completely separate times the resulting assignment was non-random with respect to time (see Figure 16).

6.1.4. Data Cleaning

Before performing any analysis the raw data ($n = 2,257$) was pruned to remove irrelevant and low-quality data points. Irrelevant data points were those coming from participants that either did not use a mouse or participated more than once ($n = 1,116$). Low-quality data points were those coming from participants with either fewer than 420 recorded observations (c.f. Section 5.2) or a browser refresh rate below 20Hz ($n = 63$). After pruning $n = 1,078$ data points were left.

6.1.5. Group Differences

Due to non-random assignment each treatment group was examined for differences that could provide alternative explanations for the results. No visually concerning between group differences were observed in screen resolution (Figure 14), web browser (Figure 14), age (Figure 15), gender (Figure 15) or pretest performance (Figure 16).

6.1.6. Hypothesis Tests

To determine the most appropriate hypothesis test the normality assumption was checked for all treatments (Figure 17). Due to deviations from normality along with the dependent variable being discrete the decision was made to use nonparametric Kruskal-Wallis and Mann-Whitney-Wilcoxon tests.

Finally, to test the hypotheses it might seem as though either performance gain (i.e.,

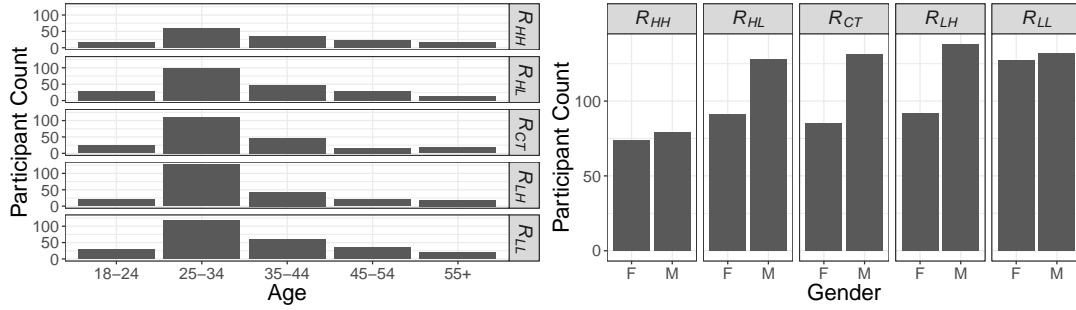


Figure 15. The age and gender distributions of participants by treatment group in Experiment 1.

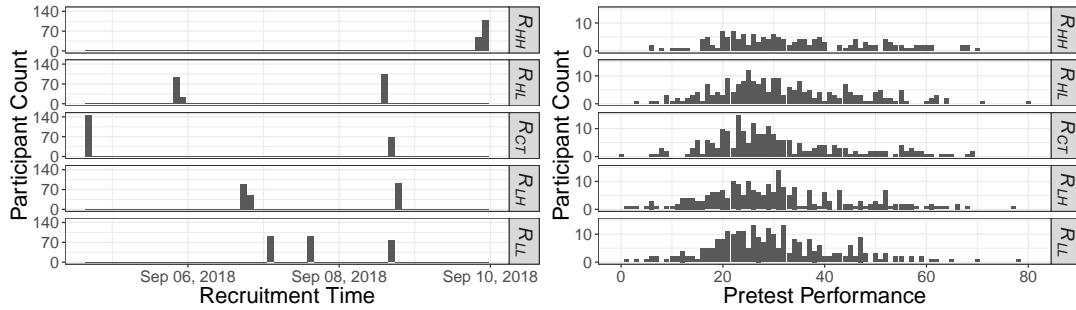


Figure 16. The recruitment times and pretest performance distributions by group in Experiment 1.

posttest performance minus pretest performance) or residual scores (i.e., residuals after predicting posttest performance from pretest performance) should be used. However, [27] has shown that both these metrics have undesirable characteristics. Therefore, all hypothesis tests are performed using simple posttest performance.

6.1.7. Results

Examining the experiment’s posttest results (provided in Table 5), the order of the treatment group means and medians (i.e., $R_{HH} > R_{HL} > R_{LH} > R_{CT} > R_{LL}$) closely align with the alternative hypothesis. A notable deviation from the hypothesis in this ordering is $R_{LH} > R_{CT}$ which was hypothesized to be $R_{CT} > R_{LH}$.

The distribution of posttest performance in all treatment groups was observed to have a rightward skew (cf. Figure 17). This was understandable considering that performance had a lower bound of 0 and no upper bound.

To visually compare posttest performance distributions to the control group Q-Q plots were generated (see Figure 18). Once again, these plots appeared to align with the hypotheses with the exception of the R_{LH} plot.

Applying the appropriate one-tailed Mann-Whitney-Wilcoxon test to each treatment group gave $H1_0$ ($p = .017$, $p = .088$) and $H2_0$ ($p = .724$, $p = .081$). Because two tests were conducted for each hypothesis a Holm-Bonferroni adjustment was applied to maintain an overall $\alpha = .05$. After the adjustment $H1_0$ was rejected for $H1_a$ with $p = .035$ while $H2_0$ failed to be rejected.

To rule out potential confounding explanations due to non-random assignment a

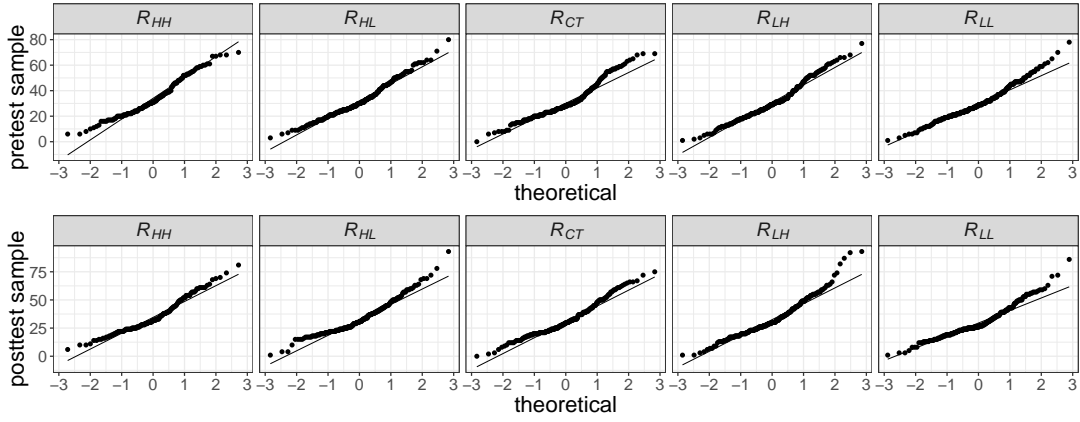


Figure 17. Q-Q plots of the dependent variables (i.e., targets touched) against a normal distribution.

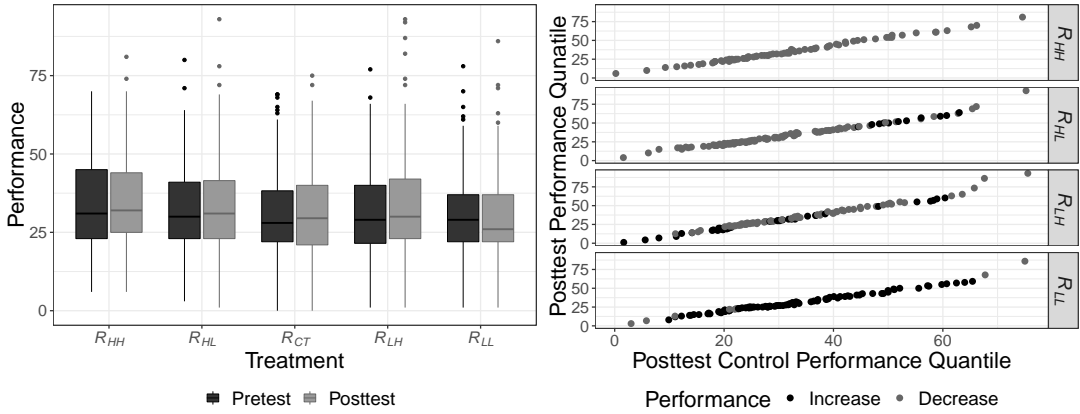


Figure 18. The left image shows boxplots of pretest/posttest performance for each group in Experiment 1. The right image shows Q-Q plots of posttest performance between treatments and control in Experiment 1.

Kruskal-Wallis test was conducted on pretest performance (cf. Figure 16). As desired, this test failed to reject the null hypothesis of no group differences ($p = .106$).

Finally, in an effort to explain the unexpected results, R_{LH} was examined more closely. It was observed that the no-touch feature expectation (cf. Table 3) for R_{LH} was closer to π_{EH} than π_{EL} . This seemed to suggest that finding a reward which delivered the desired effect, at least when learning rewards with KPIRL, was more nuanced than simply learning from a human expert exhibiting the desired behavior.

6.2. Experiment 2

6.2.1. Hypothesis

H3₀ R_{HH} feedback will not alter performance for first-time participants using a mouse

H3_a R_{HH} feedback will increase performance for first-time participants using a mouse

H4₀ R_{HL} feedback will not alter performance for first-time participants using a mouse

Table 5. Experiment 1 posttest performance statistics by treatment (with Holm-Bonferroni adjustment).

Treatment	n	Mean	Median	Var	Hypothesis	p	Cliff's d	Cliff's d 95% CI
R_{HH}	153	35.078	32	216.244	$H1_0$	0.035	0.129	(0.009, 0.244)
R_{HL}	219	33.635	31	200.508	$H1_0$	0.088	0.075	(-0.034, 0.182)
R_{LH}	231	33.022	30	248.221	$H2_0$	0.724	0.033	(-0.075, 0.139)
R_{LL}	259	29.954	26	171.649	$H2_0$	0.162	-0.074	(-0.178, 0.031)
R_{CT}	216	31.926	29.5	205.083	-	-	-	-

Table 6. These were the attributes included with all Experiment 2 AMT work requests.

Title	Play two, quick (15 second) cursor (finger) touch games
Description	Navigate to website to complete two 15 second cursor (touch) games.
Payment	\$0.10

H4_a R_{HL} feedback will increase performance for first-time participants using a mouse

H5₀ R_{LH} feedback will not alter performance for first-time participants using a mouse

H5_a R_{LH} feedback will increase performance for first-time participants using a mouse

H6₀ R_{LL} feedback will not alter performance for first-time participants using a mouse

H6_a R_{LL} feedback will decrease performance for first-time participants using a mouse

6.2.2. Recruitment

To recruit participants an AMT work request was posted using the data in Table 6. This request would have appeared on participants' devices as one option among many potential requests. In total 3,898 participants were recruited, an increase from Experiment 1 due to the small effect-sizes observed in Experiment 1.

6.2.3. Assignment

Participants were assigned to a random treatment group after recruitment. To reduce the risk of assignment bias an http request to random.org was used, when possible, to determine assignment rather than browser specific random number generators.

6.2.4. Data Cleaning

Before performing any analysis the raw data ($n = 3,898$) was pruned identically to Experiment 1 (cf. Section 6.1.4), removing irrelevant ($n = 1,783$) and low-quality ($n = 94$) data points. This left 2,021 data points for analysis. Finally, a hundred data points were randomly selected from the final data set to hand-check for accuracy. No errors were found in any of the hand-checked data points.

6.2.5. Group Differences

The group differences in Experiment 2 were similar to Experiment 1. Therefore, only the distribution of recruitment times is reproduced in Figure 19 since these changed considerably due to the change in assignment protocol. It is also worth noting that the early spike in recruitment time was the result of a small test to make sure everything was setup correctly before beginning full recruitment.

6.2.6. Hypothesis Tests

The Q-Q plots for Experiment 2 pretest/posttest performance had similar deviations from normality as seen in Figure 17 (along with performance still being discrete).

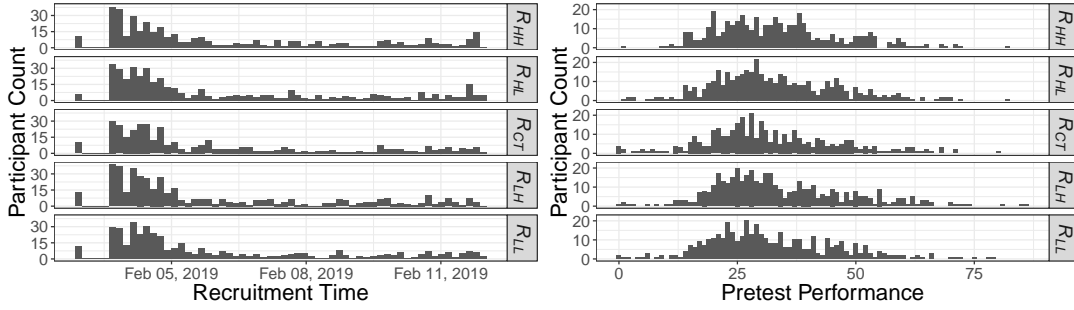


Figure 19. The recruitment times and pretest performance distributions by group in Experiment 2.

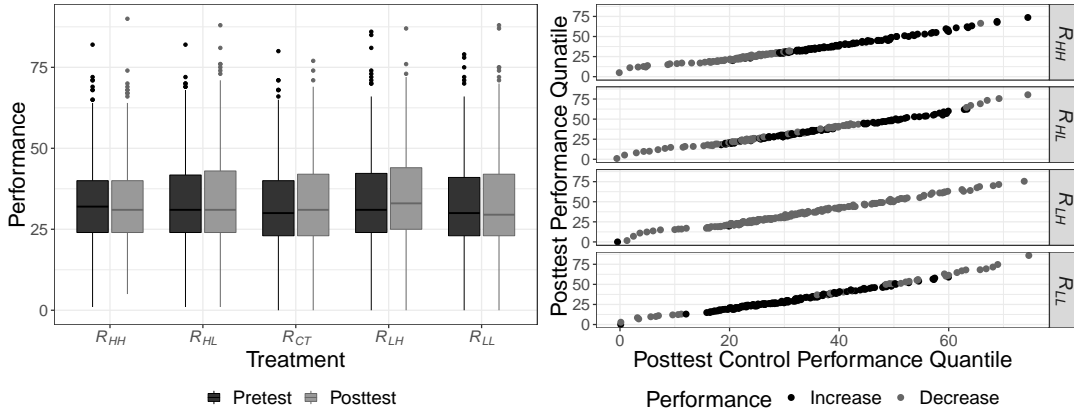


Figure 20. The left image shows boxplots of pretest/posttest performance for each group in Experiment 2. The right image shows Q-Q plots of posttest performance between treatments and control in Experiment 2.

Therefore, the same nonparametric tests on the same metrics were used in Experiment 2 as Experiment 1 (cf. Section 6.1.6).

6.2.7. Results

In Experiment 2 posttest performance summary statistics (provided in Table 7) were similar to Experiment 1 (cf. Section 6.1.7) with the exception of R_{LH} becoming the best performer and group differences becoming smaller. The order for the treatment group performance means was $R_{LH} > R_{HH} > R_{HL} > R_{CT} > R_{LL}$ and for the treatment group performance medians was $R_{LH} > R_{HH} = R_{HL} = R_{CT} > R_{LL}$.

The Kruskal-Wallis applied to pretest performance still failed to reject the null ($p = .217$). The Mann-Whitney-Wilcoxon test rejected the null for H_{5_0} ($p = .034$) while failing to reject the null for H_{3_0} ($p = .374$), H_{4_0} ($p = .365$) and H_{6_0} ($p = .279$). No Holm-Bonferroni adjustment was applied this time since only one test was conducted for each hypothesis.

Failing to reject the null for so many rewards after increasing sample size was disappointing but not completely unexpected given the use of random assignment to statistically remove unintended between group differences. It was considered promising that all effect sizes still pointed in the same direction as Experiment 1, even if they were weaker. Taken together the results seemed to support the overall conjecture while

Table 7. Experiment 2 posttest performance statistics by treatment (sans Holm-Bonferroni adjustment).

Treatment	n	Mean	Median	Var	Hypothesis	p	Cliff's d	Cliff's d 95% CI
R_{HH}	399	33.426	31.0	166.155	$H3_0$	0.374	0.013	(-0.069, 0.095)
R_{HL}	418	33.653	31.0	196.002	$H4_0$	0.365	0.014	(-0.067, 0.095)
R_{LH}	432	35.130	33.0	208.368	$H5_0$	0.034	0.075	(-0.006, 0.154)
R_{LL}	402	33.035	29.5	222.044	$H6_0$	0.279	-0.024	(-0.106, 0.057)
R_{CT}	370	33.114	31.0	205.911	-	-	-	-

suggesting more careful reward design needs to be considered to achieve the desired results.

7. Conclusion

This paper started with a simple question: could an IRL reward function learned from human experts provide feedback on a task to predictably alter the performance of future human participants.

To test this idea two new algorithms were developed: *KPIRL* and *KLA*. Both algorithms outperformed previously published research within the RL and IRL community when applied to a large state-spaces with nonlinear reward functions. However, three open research questions remain with these algorithms:

- (1) Can KPIRL be modified to output a single optimal reward rather than a set?
- (2) What performance bounds and characteristics does KLA possess?
- (3) Can recent work in [40] be adapted to improve on the OSA algorithm used above?

In addition to the algorithms two human subject experiments were conducted to measure the effect of IRL reward function feedback on human performance. To the best of the authors' knowledge this was the first such experiment testing the efficacy of IRL for an FI. Towards this end, there are three areas that should be explored further:

- (1) What, if any, principles govern how reward functions influence human behavior
- (2) What, if any, effect does this technique have on long-term performance/learning
- (3) What domains are best suited for human to human feedback interventions

In conclusion, the effect sizes of the experiments were small but significant. The results were seen as even more of a success given that experiments were not conducted in a controlled lab setting, but rather on remote devices in uncontrolled environments by unknown participants. There remains room for improvement, but all these improvements appear to be within the reach of current technology and experimental methods.

Acknowledgements

This project was made possible in part through the support of the University of Virginia Data Science Institute, with funding from the Presidential Fellowship in Data Science.

References

- [1] Pieter Abbeel and Andrew Y Ng. “Apprenticeship learning via inverse reinforcement learning”. In: *Proceedings of the twenty-first international conference on Machine learning*. ACM. 2004, p. 1.
- [2] Pieter Abbeel et al. “An application of reinforcement learning to aerobatic helicopter flight”. In: *Advances in neural information processing systems*. 2007, pp. 1–8.
- [3] Nachman Aronszajn. “Theory of reproducing kernels”. In: *Transactions of the American mathematical society* 68.3 (1950), pp. 337–404.
- [4] Albert Bandura, Dorothea Ross, and Sheila A Ross. “Transmission of aggression through imitation of aggressive models.” In: *The Journal of Abnormal and Social Psychology* 63.3 (1961), p. 575.
- [5] Pierre Bernhard. “Information and strategies in dynamic games”. In: *SIAM Journal on Control and Optimization* 30.1 (1992), pp. 212–228.
- [6] Dimitri P Bertsekas. “Approximate policy iteration: A survey and some new methods”. In: *Journal of Control Theory and Applications* 9.3 (2011), pp. 310–335.
- [7] David Blackwell. “Discounted dynamic programming”. In: *The Annals of Mathematical Statistics* 36.1 (1965), pp. 226–235.
- [8] Justin A Boyan. “Technical update: Least-squares temporal difference learning”. In: *Machine learning* 49.2-3 (2002), pp. 233–246.
- [9] Lora E Burke, Jing Wang, and Mary Ann Sevick. “Self-monitoring in weight loss: a systematic review of the literature”. In: *Journal of the American Dietetic Association* 111.1 (2011), pp. 92–102.
- [10] Jaedeug Choi and Kee-Eung Kim. “Bayesian Nonparametric Feature Construction for Inverse Reinforcement Learning.” In: *IJCAI*. 2013, pp. 1287–1293.
- [11] Christoph Dann, Gerhard Neumann, and Jan Peters. “Policy evaluation with temporal differences: A survey and comparison”. In: *The Journal of Machine Learning Research* 15.1 (2014), pp. 809–883.
- [12] Mahmoud Elnaggar and Nicola Bezzo. “An IRL approach for cyber-physical attack intention prediction and recovery”. In: *2018 Annual American Control Conference (ACC)*. IEEE. 2018, pp. 222–227.
- [13] Abraham P George and Warren B Powell. “Adaptive stepsizes for recursive estimation with applications in approximate dynamic programming”. In: *Machine learning* 65.1 (2006), pp. 167–198.
- [14] John Hattie and Helen Timperley. “The power of feedback”. In: *Review of educational research* 77.1 (2007), pp. 81–112.
- [15] Sander Hermsen et al. “Using feedback through digital technology to disrupt and change habitual behavior: A critical review of current literature”. In: *Computers in Human Behavior* 57 (2016), pp. 61–74.
- [16] Beomjoon Kim and Joelle Pineau. “Socially adaptive path planning in human environments using inverse reinforcement learning”. In: *International Journal of Social Robotics* 8.1 (2016), pp. 51–66.
- [17] Edouard Klein et al. “A cascaded supervised learning approach to inverse reinforcement learning”. In: *Joint European Conference on Machine Learning and Knowledge Discovery in Databases*. Springer. 2013, pp. 1–16.
- [18] Avraham N Kluger and Angelo DeNisi. “The effects of feedback interventions on performance: A historical review, a meta-analysis, and a preliminary feedback intervention theory.” In: *Psychological bulletin* 119.2 (1996), p. 254.

- [19] Henrik Kretzschmar et al. “Socially compliant mobile robot navigation via inverse reinforcement learning”. In: *The International Journal of Robotics Research* 35.11 (2016), pp. 1289–1307.
- [20] Michail G Lagoudakis and Ronald Parr. “Least-squares policy iteration”. In: *Journal of machine learning research* 4.Dec (2003), pp. 1107–1149.
- [21] Kamwo Lee et al. “Agent-based model construction using inverse reinforcement learning”. In: *Simulation Conference (WSC), 2017 Winter*. IEEE. 2017, pp. 1264–1275.
- [22] Matthew L Lee and Anind K Dey. “Real-time feedback for improving medication taking”. In: *Proceedings of the 32nd annual ACM conference on Human factors in computing systems*. ACM. 2014, pp. 2259–2268.
- [23] Sergey Levine, Zoran Popovic, and Vladlen Koltun. “Feature construction for inverse reinforcement learning”. In: *Advances in Neural Information Processing Systems*. 2010, pp. 1342–1350.
- [24] Sergey Levine, Zoran Popovic, and Vladlen Koltun. *IRL Toolkit*. 2011. URL: <http://graphics.stanford.edu/projects/gpir1/index.htm> (visited on 10/23/2019).
- [25] Sergey Levine, Zoran Popovic, and Vladlen Koltun. “Nonlinear inverse reinforcement learning with gaussian processes”. In: *Advances in Neural Information Processing Systems*. 2011, pp. 19–27.
- [26] Rebecca Lewthwaite and Gabriele Wulf. “Social-comparative feedback affects motor skill learning”. In: *The Quarterly Journal of Experimental Psychology* 63.4 (2010), pp. 738–749.
- [27] Robert L Linn and Jeffrey A Slinde. “The determination of the significance of change between pre-and posttesting periods”. In: *Review of Educational Research* 47.1 (1977), pp. 121–150.
- [28] Jun Ma and Warren B Powell. “Convergence analysis of kernel-based on-policy approximate policy iteration algorithms for markov decision processes with continuous, multidimensional states and actions”. In: *Submitted to IEEE Transactions on Automatic Control* (2010).
- [29] Kaisu Mononen et al. “The effects of augmented kinematic feedback on motor skill learning in rifle shooting”. In: *Journal of sports sciences* 21.10 (2003), pp. 867–876.
- [30] Dan Morris et al. “Haptic feedback enhances force skill learning”. In: *Second Joint EuroHaptics Conference and Symposium on Haptic Interfaces for Virtual Environment and Teleoperator Systems (WHC’07)*. IEEE. 2007, pp. 21–26.
- [31] A Nedić and Dimitri P Bertsekas. “Least squares policy evaluation algorithms with linear function approximation”. In: *Discrete Event Dynamic Systems* 13.1-2 (2003), pp. 79–110.
- [32] Andrew Y Ng, Stuart J Russell, et al. “Algorithms for inverse reinforcement learning.” In: *Icml*. 2000, pp. 663–670.
- [33] Elnaz Nouri, Kallirroi Georgila, and David Traum. “A cultural decision-making model for negotiation based on inverse reinforcement learning”. In: *Proceedings of the Annual Meeting of the Cognitive Science Society*. 2012.
- [34] Warren B Powell. *Approximate Dynamic Programming: Solving the Curses of Dimensionality, 2nd Edition*. John Wiley & Sons, 2011.
- [35] Qifeng Qiao and Peter A Beling. “Inverse reinforcement learning with gaussian process”. In: *American Control Conference (ACC), 2011*. IEEE. 2011, pp. 113–118.

- [36] Deepak Ramachandran and Eyal Amir. “Bayesian inverse reinforcement learning”. In: *Urbana* 51.61801 (2007), pp. 1–4.
- [37] Nathan D Ratliff, J Andrew Bagnell, and Martin A Zinkevich. “Maximum margin planning”. In: *Proceedings of the 23rd international conference on Machine learning*. ACM. 2006, pp. 729–736.
- [38] Nicholas Rhinehart and Kris M Kitani. “First-person activity forecasting with online inverse reinforcement learning”. In: *Proceedings of the IEEE International Conference on Computer Vision*. 2017, pp. 3696–3705.
- [39] Herbert Robbins and Sutton Monro. “A stochastic approximation method”. In: *The annals of mathematical statistics* (1951), pp. 400–407.
- [40] Ilya O Ryzhov, Peter I Frazier, and Warren B Powell. “A new optimal stepsize for approximate dynamic programming”. In: *IEEE Transactions on Automatic Control* 60.3 (2014), pp. 743–758.
- [41] Bernhard Scholkopf and Alexander J Smola. *Learning with kernels: support vector machines, regularization, optimization, and beyond*. MIT press, 2001.
- [42] Dale H Schunk and Carl W Swartz. “Goals and progress feedback: Effects on self-efficacy and writing achievement”. In: *Contemporary educational psychology* 18.3 (1993), pp. 337–354.
- [43] Valerie J Shute. “Focus on formative feedback”. In: *Review of educational research* 78.1 (2008), pp. 153–189.
- [44] David Silver et al. “Mastering the game of go without human knowledge”. In: *Nature* 550.7676 (2017), p. 354.
- [45] Ralph E Strauch. “Negative dynamic programming”. In: *The Annals of Mathematical Statistics* 37.4 (1966), pp. 871–890.
- [46] Richard S Sutton and Andrew G Barto. *Reinforcement learning: An introduction*. MIT press, 2018.
- [47] Amos Tversky and Daniel Kahneman. “Loss aversion in riskless choice: A reference-dependent model”. In: *The quarterly journal of economics* 106.4 (1991), pp. 1039–1061.
- [48] Richard K Wagner. “Tacit knowledge in everyday intelligent behavior.” In: *Journal of personality and social psychology* 52.6 (1987), p. 1236.
- [49] Christopher JCH Watkins and Peter Dayan. “Q-learning”. In: *Machine learning* 8.3-4 (1992), pp. 279–292.
- [50] Christopher John Cornish Hellaby Watkins. “Learning from delayed rewards”. In: (1989).
- [51] Gabriele Wulf, Charles H Shea, and Sabine Matschiner. “Frequent feedback enhances complex motor skill learning”. In: *Journal of motor behavior* 30.2 (1998), pp. 180–192.
- [52] Gabriele Wulf, Charles Shea, and Rebecca Lewthwaite. “Motor skill learning and performance: a review of influential factors”. In: *Medical education* 44.1 (2010), pp. 75–84.
- [53] Markus Wulfmeier et al. “Large-scale cost function learning for path planning using deep inverse reinforcement learning”. In: *The International Journal of Robotics Research* 36.10 (2017), pp. 1073–1087.
- [54] Xin Xu, Dewen Hu, and Xicheng Lu. “Kernel-based least squares policy iteration for reinforcement learning”. In: *IEEE Transactions on Neural Networks* 18.4 (2007), pp. 973–992.
- [55] Brian D Ziebart et al. “Maximum Entropy Inverse Reinforcement Learning.” In: *AAAI*. Vol. 8. Chicago, IL, USA. 2008, pp. 1433–1438.

- [56] Brian D Ziebart et al. “Navigate like a cabbie: Probabilistic reasoning from observed context-aware behavior”. In: *Proceedings of the 10th international conference on Ubiquitous computing*. ACM. 2008, pp. 322–331.
- [57] Brian Ziebart, Anind Dey, and J Andrew Bagnell. “Probabilistic pointing target prediction via inverse optimal control”. In: *Proceedings of the 2012 ACM international conference on Intelligent User Interfaces*. ACM. 2012, pp. 1–10.